The Structure Function Relationship of Disordered Networks using Young's Modulus and Floppy Modes

Melinda Tajnai, Hilary Jacks

Department of Physics, California Polytechnic State University, San Luis Obispo

Abstract

Disordered networks may have the ability to store information that can be retrieved using a Young's modulus measurement. The effect of the number of floppy modes a network has on the value of this Young's modulus measurement is unknown. This experiment uses 28 networks consisting of 3D printed edges in a sliding frame to determine how the Young's modulus of a network is related to the number of floppy modes.

I. Introduction

Disordered networks may show varying levels of rigidity depending on how internal constraints are distributed within the network [1] [2]. Networks can be classified as isostatic, hypostatic, or hyperstatic depending on the relative numbers of constraints and degrees of freedom [1]. An isostatic network will have exactly the same number of constraints as there are degrees of freedom [1]. Networks that do not have equal numbers of constraints and degrees of freedom are called hypostatic and hyperstatic which correspond to a greater number of degrees of freedom and a greater number of constraints, respectively [1]. These constraints are often counted using a Maxwell count which is a way to quantify the number of floppy modes a network has.

Disordered systems have the ability to store information; the information can often be read using a measurement of a bulk property like the Young's modulus [3] [4]. There is also interest in the switching behavior of isostatic regions in larger networks between configurations that are energetically degenerate. Which configuration the isostatic region is in may be able to be read out using a Young's modulus or bulk modulus measurement. However, it is unknown to what extent this Young's modulus measurement is dependent on the number of floppy modes outside of the isostatic region. Floppy modes account for the internal and translational degrees of freedom the network has due to the way these edges are arranged; it is unclear whether the floppy modes or number of edges present in a given network is a better determinant of its rigidity [1] [2].

In this exploration we will physically build and examine a set of networks and compare their number of floppy modes to the measured Young's modulus of the network to see if there is a clearly defined relationship between these parameters. If a clear relationship between the Young's modulus of the network and the rigidity of the network as described by the number of floppy modes exists, we can hope to discover more about how rigidity and specific edge-node configurations affect

Unit of Disordered Network

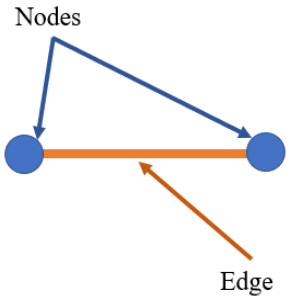

Small Disordered Network

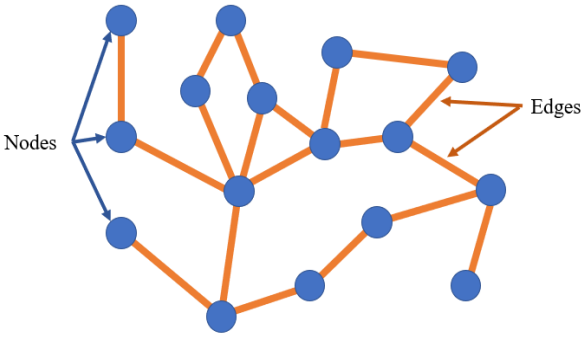

Figure 1: The figure above shows a single edge terminated on each end by a node and a small disordered network made up of many edges and nodes.

bulk properties like the Young's modulus. Furthermore, if an empirical relationship exists between the number of floppy modes and the Young's modulus, networks or materials that cannot be viewed directly to compute a Maxwell count may benefit from using a measure of Young's modulus to learn more about the rigidity of the material.

II. Methods

The disordered system in this experiment can be described as a network of edges and nodes. Edges and nodes can be visualized simply as straight lines (edges) that connect at points (nodes) or as atoms (nodes) and bonds between atoms (edges). A diagram of these edges and nodes is shown in *Figure 1*.

The networks used in this experiment were part of a larger network that was created by Dr. Varda Hagh. The network consisted of a large number of edges and nodes that were configured to be maximally constrained. A small region consisting of 34 edges connected at 16 nodes was selected as a base for all networks. From this base network, edges were removed one at a time to create the set of 34 networks studied here. All networks with greater than 28 edges required too many edges to attach to singular nodes which forced the network out of a single plane and therefore could not be examined in this experiment. Therefore, only networks with 28 or fewer edges were physically built and examined for this study. The 28 networks that were constructed for this exploration are diagrammed in *Figure 2*.

We use floppy modes to quantify the rigidity of the networks in this study. The number of floppy modes a network has is a measure of the number of degrees of freedom that has been corrected to remove redundancies in the structure. There are several forms of this equation in the literature [1] [2], but for this examination we will use the condensed version shown below as equation 1,

$$F = dN_E - N_R \qquad (1)$$

where d is the number of dimensions the network exists in, N_E is the number of edges in the network, and N_R is the number of redundant edges in the network [1]. In

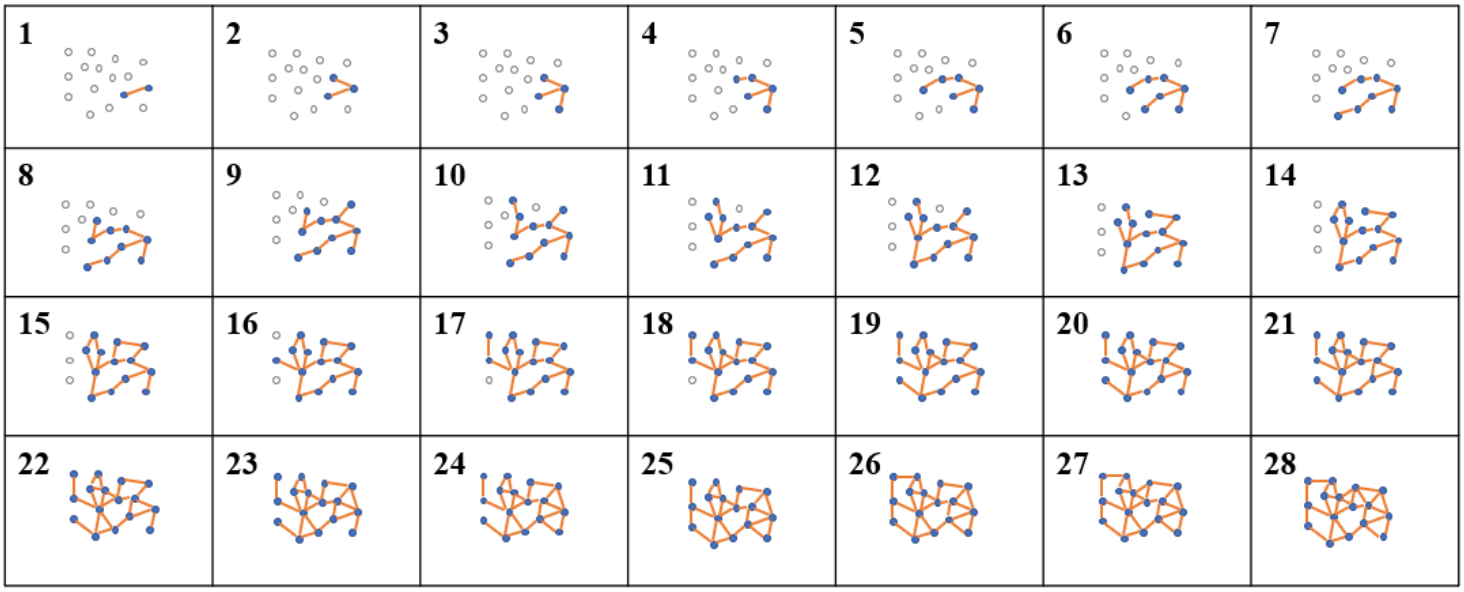

Figure 2: The figure above shows the set of networks to be constructed in this exploration. Each node is represented by a blue dot and each edge is shown as an orange line.

this case, d=2 as all networks were constructed in two dimensions. Computing a Maxwell count for a given network involves counting the number of degrees of freedom a network has while also subtracting any constraints that limit the number of degrees of freedom [1] [2].

Redundant edges pose difficulties to counting the number of floppy modes as many different methods of determining which edges are redundant exist. [5]. Furthermore, Maxwell counts, the practice of counting restraints to determine how constrained a network is [2], are only considered correct when the networks constraints are independent or are corrected for [1] [2]. For the networks in this experiment, the number of redundant edges was found using the minimum spanning tree of the networks. A minimum spanning tree of a network only includes the minimum number of edges needed to connect all nodes of the network without forming loops or cycles. The number of edges not included in the minimum spanning tree can be said to be redundant because the edges form internal cycles or loops within the network and removing these edges will not affect the connectedness of the network. The algorithm used to find the minimum spanning tree of every network in this experiment is Kruskal's algorithm. Kruskal's algorithm consists of two phases: the sorting phase and the set-union phase [6] [7]. The sorting phase gathers together all edges within the network in the order they were drawn and the set-union phase adds in edges one by one, removing any edges that form cycles, to create the minimum spanning tree [6] [7]. Using the online tool at visualgo.net/en/mst, each network was drawn and the algorithm was run to calculate the minimum spanning tree. When the algorithm finished analyzing the network, all redundant edges were greyed out and counted to be used in the calculation of floppy modes. Equation 1 was used to compute the number of floppy

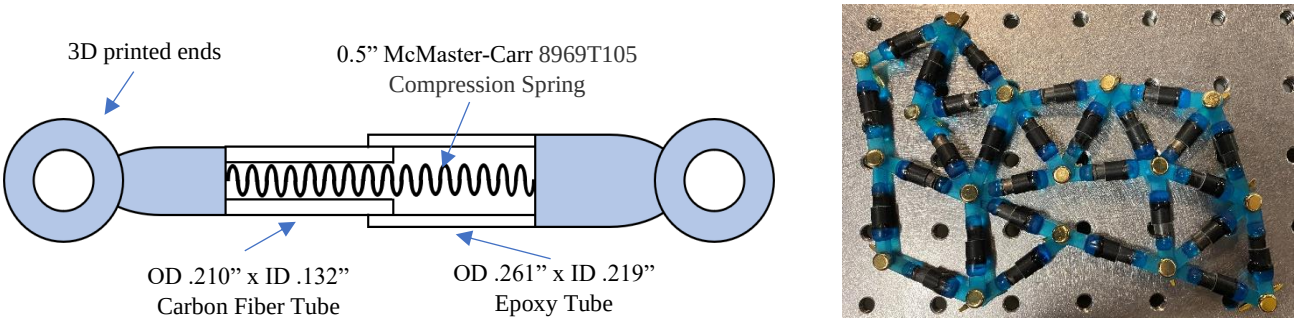

Figure 3: The figure above shows the final design for the spring like edges. The left image shows a diagram of an individual edge. The right image shows an example of a network constructed using these edges.

modes for all networks examined in this exploration.

The first step to start building these networks was to construct the spring-like edges. These edges need to both change in length with a spring-like restoring force and remain straight throughout this length change. The design of these edges underwent many iterations before arriving at a final design. Previous iterations included combinations of compression and extension springs with 3D printed pieces which proved difficult to fine tune and resource intensive to construct. The final design is diagrammed in *Figure 3*. The edges were 3D printed using a FormLabs Form 2 Stereolithography 3D printer and FormLabs Tough Resin V5. The resin underwent a final curing step in a modified eyeglass UV sterilization cabinet. Any remaining support structures that were not completely removed after the final cure step were filed down using small round metal files. Each 3D printed edge end is affixed to a 0.3in long piece of carbon fiber tubing or epoxy tubing that matches the outer diameter of the 3D printed end. Within each edge a 0.5” long stainless-steel spring with a rate of 2.08 lbs/in is installed using a UV resin adhesive. In total, 28 edges were used to construct the set of networks. All edges are identical in construction. Edges were

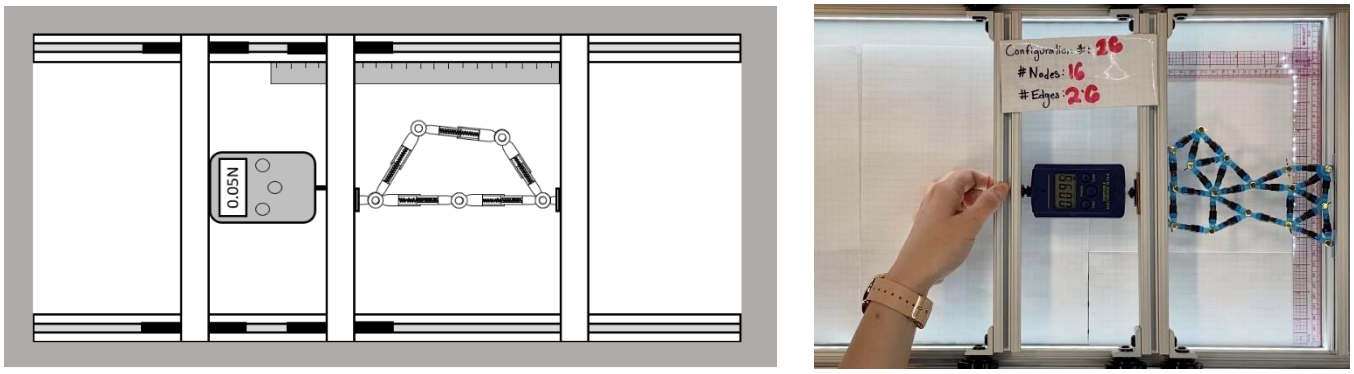

Figure 4: The figure above shows the experimental setup used to test the networks. The right-most vertical bar is stationary. The middle and left rail are on a set of wheels that allow them to smoothly slide. A small force sensor is attached to the two rolling rails and the length between these rolling rails is fixed. The two horizontal rails provide channels along which the wheels roll smoothly. The network being analyzed is inserted between the middle rolling rail and the right stationary rail. Rulers are used track how far the network stretches.

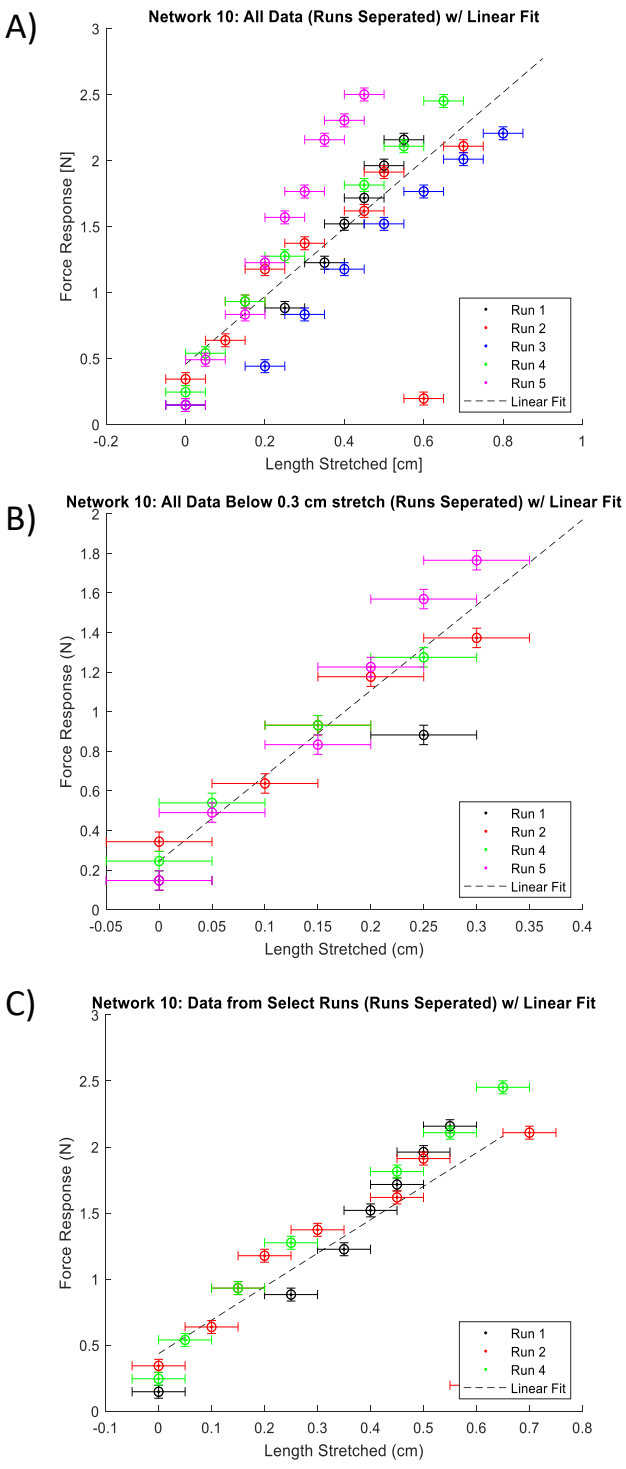

Figure 5: A) All data collected for Network 10. B) Data collected for Network 10 with run 3 omitted and length stretched restricted to less than 0.3 cm. C) All data for runs 1, 2, and 4 for Network 10.

connected together loosely to avoid excessive friction using metal tacks.

The experimental setup includes a frame in which to mount the network to be analyzed, a force sensor to measure the networks response to being stretched, and a method to record the change in length of the network. The frame that was constructed is detailed in *Figure 4*. The frame was constructed using 1 inch T-slotted aluminum framing rails that were bolted together using L brackets. Two long 3- foot T-slotted rails were used for the top and bottom primary sliding rails. The sliding portion of the frame used 1-inch slotted wheels made to slide along the T-slotted rails. A force sensor was affixed between the two rolling rails using superglue. The inside rail slot was lined with an LED strip to illuminate the workspace and make the rulers used for data collection visible in the data videos.

The experimental setup is placed below a camera and a video of the network being stretched is recorded for several trials. The measured force and change in size of the network is recorded. This is repeated for five runs for each of the 28 networks. In total, 148 videos were recorded for analysis. Each video is then viewed, and the length of the network and the force exerted by the network at that length is recorded. All of the individual runs are compiled into one plot of reaction force versus length stretched and a linear fit is used to find the Young's Modulus of each of the networks. The Young's Modulus in this 2D case reduces to units of N/m [8].

A major issue that arose when analyzing the data collected was that the data did not always follow a strictly linear regime.

Because the analysis here relies on fitting the data to a linear equation, several different analysis methods were used to isolate the linear regions of data to use in the calculation of Young's modulus. The first method used made no considerations for the linearity of the data and a linear fit was found using all data points from all trials. The second method used only select trials for each network, omitted trials with identifiable issues, and restricted the data to extensions of less than 0.3 cm from the relaxed length. The identifiable issues included overextension of edges, edges becoming stuck and not extending correctly, or edges that had been stuck but were released during the trial. The final method used select trials for each network and omitted trials where there were identifiable issues without restricting the extension length. An example of how these analysis methods varied for network 10 is shown in *Figure 5.*

After each network was plotted using all three analysis methods, the data was fit to a line using the standard linear formula $y = mx + b$ where the slope m was the calculated Young's modulus value. All data for a given analysis method was compiled into a plot of Young's modulus vs. floppy modes. The plots generated for all three analysis methods are shown in *Figure 6.*

III. Results and Discussion

Data analysis method 1 returned the most data points as no networks or individual runs were omitted for analysis. Because no runs were omitted, the uncertainties in the Young's modulus calculations for the networks with F=2 and F=4 are much

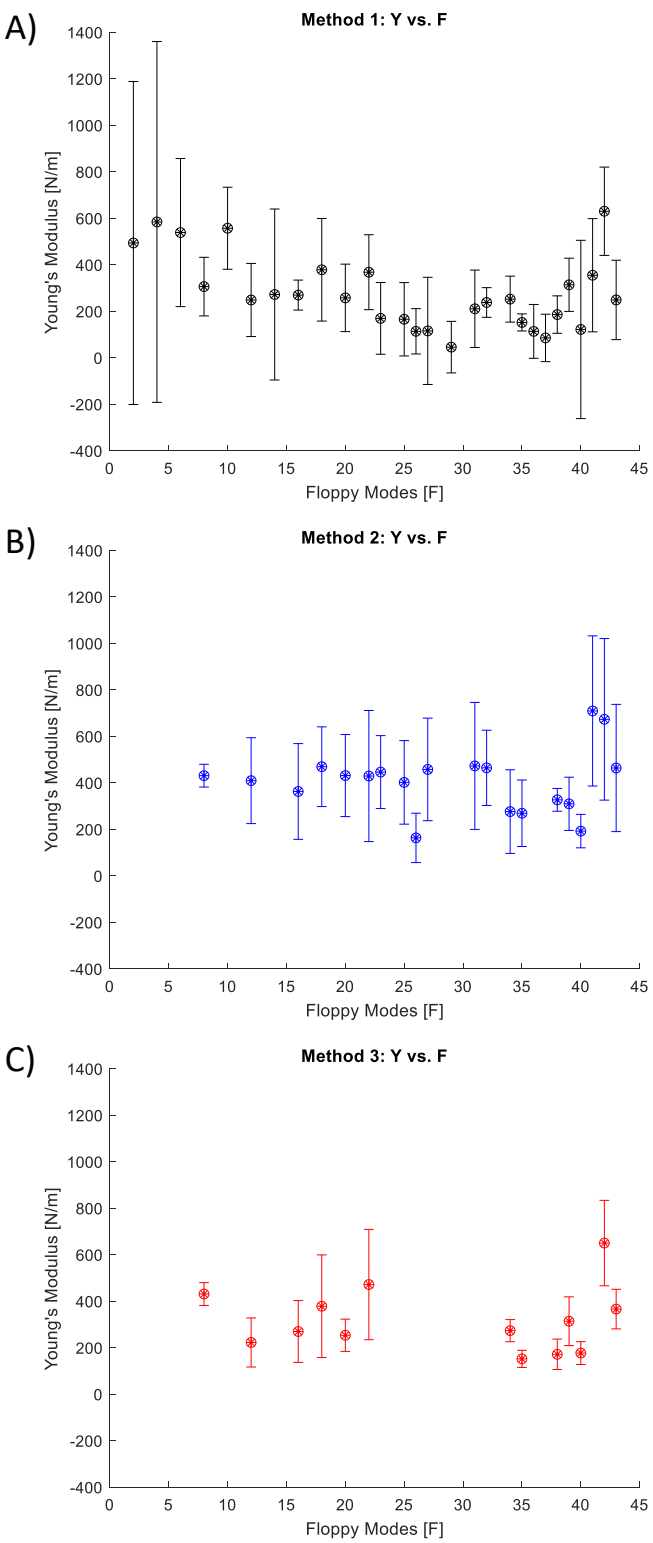

Figure 6: A) Young's modulus values computed using analysis method 1. B) Young's modulus values computed using method 2. C) Young's Modulus values computed using method3.

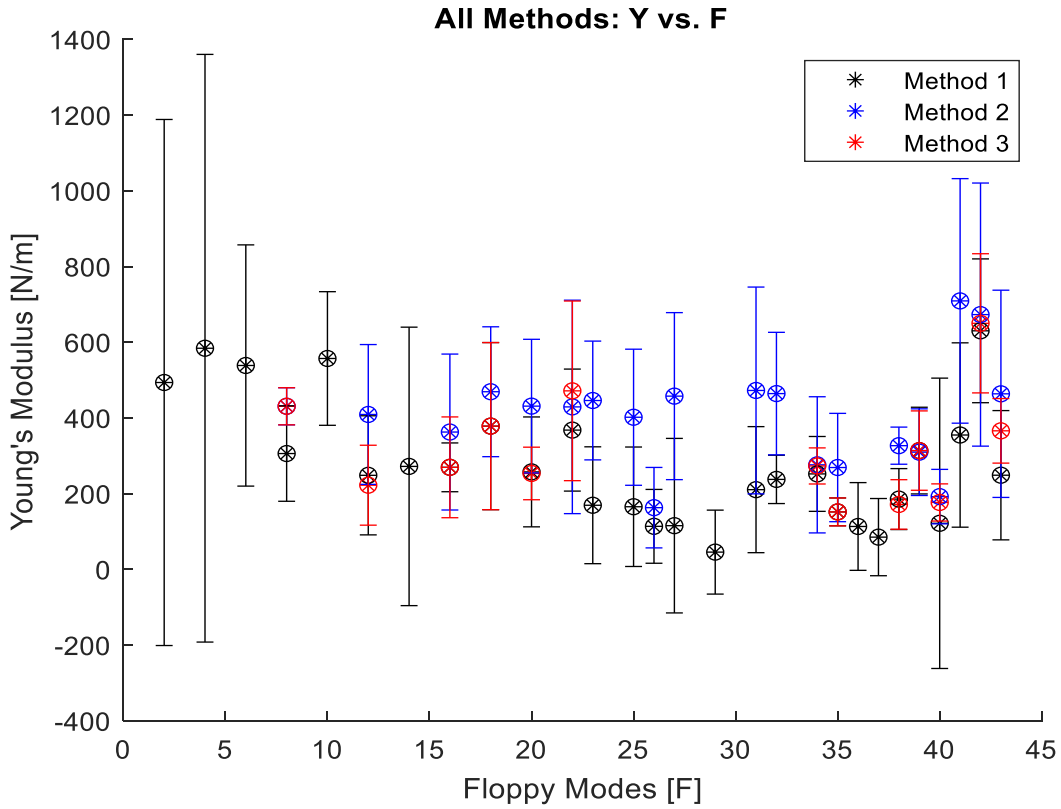

Figure 7: All calculated values of Young's Modulus for all analysis methods.

larger than any other Young's modulus uncertainty across all methods. Method 2 captured a majority of the networks examined in this exploration. While the uncertainties are much smaller than the largest seen using Method 1, they still span large value ranges for the Young's modulus. Method 3 returned the smallest uncertainties overall but also had the most limited range of networks examined as most of the networks had to be omitted from this method due to a lack of linear data across the entire extension length because of the issues described previously.

Figure 7 shows all three analysis methods. Presenting the data in this manor has little impact on illuminating a trend between the Young's modulus of a network and the number of floppy modes a network has. While the data may show a vague parabolic shape, the uncertainties of many of the values make it impossible to confidently and explicitly state that there is a meaningful relationship between these parameters.

The uncertainties present in this data likely come from several sources including springs within the edges being extended outside of their harmonic range and deforming, subtle differences in individual constructed edges, imperfections in the experimental frame construction and use, and a rush to compile as much data as possible as mass closures began due to COVID-19.

IV. Conclusion

At this time there is no conclusive result that can be derived from the data collected in this experiment. There is too much

uncertainty in the data to confidently present an empirical relationship between the two parameters in question.

Future research may benefit from repeating this process on the same set or a similar set of networks. Research can also look at larger networks with more edges and nodes or networks with different layouts. The materials used to construct the networks could also be changed or modified to have more internal consistency; edge designs may be modified, or new edges may be designed, or networks could be laser cut or 3D printed in their entirety instead of building edges individually. Finally, these networks may be simulated under the same conditions done in this experiment.

V. References

1. M.F.Thorpe, "Flexibility and Mobility in Networks," *Encyclopedia of Complexity and Systems Science*, Springer, pp. 6013- 6023, 2009.

2. M.F.Thorpe, "Bulk and Surface Floppy Modes," *Journal of Non-Crystalline Solids*, Vol. 182, Elsevier, pp. 135-142, 1995.

3. N. Keim, "Memory Formation in Matter," *Rev. Mod. Phys*, Vol. 91, 2019

4. N.Keim, "Global Memory from Local Hysteresis in an Amorphous Solid," *Physical Review Research*, Vol. 2, pp.012004-1 – 012004-6, 2020.

5. J.C.Phillips, "Constraint Theory, Vector Percolation and Glass Formation," *Solid State Communications*, Vol. 53, No. 8, pp.699-702, 1985.

6. G. Amato, G. Cattaneo, and G F. Italion, "Experimental Analysis of Dynamic Minimum Spanning Tree Algorithms (Extended Abstract)," In Proceedings of the 8th Annual ACM-SIAM Symposium on Discrete Algorithms. ACM, New York, pp. 314-323.

7. B. M. E. Moret and H. D. Shapiro, "An Empirical Analysis of Algorithms for Constructing a Minimum Spanning Tree," 1995.

8. O. Amsellem, "Two-dimensional (2D) and three-dimensional (3D) analyses of plasma-sprayed alumina microstructures for finite-element simulation of Young's modulus" *J Matter Sci*, Vol. 43, pp. 4091-4098, 2008.

VI. Appendix

i. 3D models of edge ends used for 3D printing

a. Edge End 1

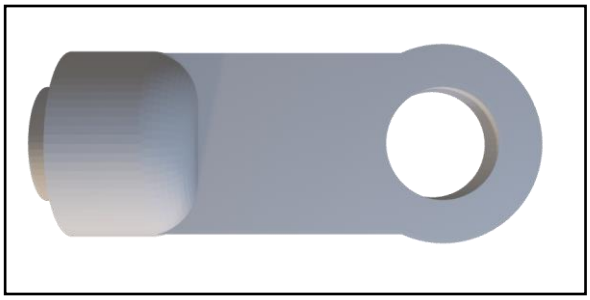

b. Edge End 2

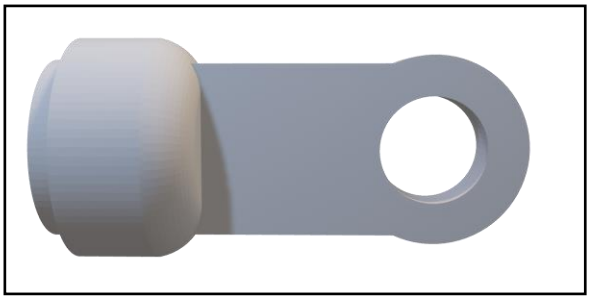

ii. Diagrams of edge ends

a. End 1 Diagram

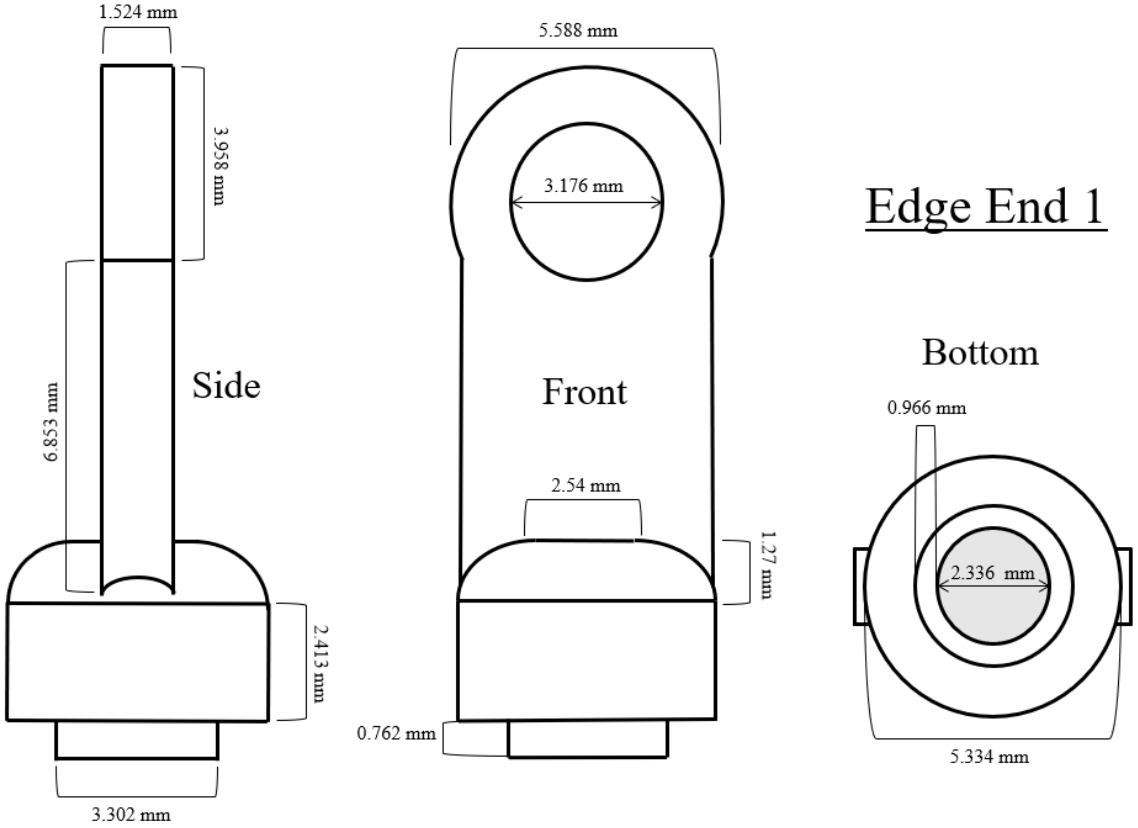

b. End 2 Diagram